ACS APPLIED MATERIALS & INTERFACES

Research Article

www.acsami.org

Doped Carbon Nanotube Networks for Electrochemical Filtration of Aqueous Phenol: Electrolyte Precipitation and Phenol Polymerization

Guandao Gao[†,‡] and Chad D. Vecitis*[,†]

[†]School of Engineering and Applied Sciences, Harvard University, Cambridge, Massachusetts 02138, United States

[‡]Key Laboratory of Pollution Processes and Environmental Criteria (Ministry of Education), College of Environmental Science and Engineering, Nankai University, Tianjin 300071, China

Supporting Information

ABSTRACT: Electrochemical filtration with anodic carbon nanotube (CNT) networks is reported to be effective for chemical and microbiological water treatment. Here, we investigate how CNT doping affects the electrochemical filtration performance toward the remediation of aromatic wastewaters. Purified and well-characterized undoped (C-CNT), boron-doped (B-CNT), and nitrogen-doped (N-CNT) anodic carbon nanotube networks are challenged with aqueous phenol in a sodium sulfate electrolyte. Steady-state current and effluent total organic carbon (TOC) measurements are utilized to evaluate the oxidative performance as a function of voltage and electrolysis time. In terms of steady-state TOC removal, at an applied voltage of 3 V all three anodic CNT networks are able to remove approximately 7 to 8 mgC L^{-1} of the influent TOC within the ~1 s liquid residence time of the electrochemical filter. The anodic CNT networks are partially passivated over the 5 h electrolysis time with the B-CNT network displaying the least passivation. The extent of passivation was observed to be inversely correlated to the CNT work function. SEM, XPS, and TGA of the electrolyzed CNT networks are used to identify the two primary passivation mechanisms of electrochemical phenols polymerization and electrochemical electrolyte precipitation. In agreement with chronoamperometry results, the B-CNT network has the lowest extent of passivating polymer and precipitate formation. The precipitant is determined to likely be sodium persulfate or carbonate and is removed with a simple acidic water wash. The polymer is determined to likely be polyphenylene oxide and is partially removed with the wash. All three anodic CNT networks display potential for energy efficient electrochemical filtration of aromatic wastewaters and the B-CNT are determined to be the most resistant to passivation.

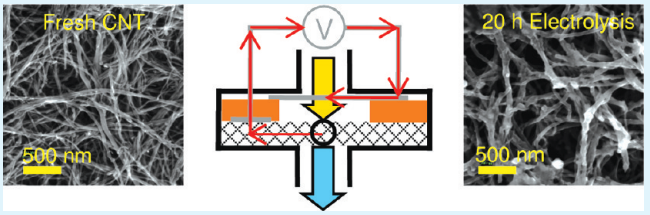

KEYWORDS: *electrochemical filtration, carbon nanotubes (CNT), water, phenol, passivation*

INTRODUCTION

Electrochemistry is utilized in many energy and environmental applications such as supercapacitors, electrochromics, electro-sensors, batteries, thermocells, and fuel cells.[1] Often overlooked is the application of electrochemistry for advanced water treatment.[2] Recent development of anodes with optimized electrocatalytic activity, high oxygen overpotentials, and extended operational lifetimes has led to electrochemical energy efficiencies that are comparable to conventional wastewater and drinking water treatment technologies.[3,4] Electrochemical water treatment efficiencies may be increased further by utilization of the aqueous waste as a sacrificial electron donor for simultaneous hydrogen production.[5]

Further advances in electrochemical water treatment performance will be made by investigating novel electrode materials and structures. One prominent area of current research is three-dimensional electrode nanoarchitechtures.[6−9] The enhanced performance of three-dimensional electrodes arises from the high surface area increasing the number of electrochemically active surface sites[7] and high porosity for enhanced ion and molecular transport.[10] The production of a three-dimensional nanoporous electrode requires that the material be electrically conducting, mechanically sound, and corrosively stable. Carbon nanotubes (CNTs) meet those requirements and are easily formed into stable, porous, and conductive networks.[7,11] Recently, a CNT network has been utilized as an anodic water filter and shown to be effective for aromatic dye, e.g., methylene blue and methyl orange, and anion, e.g., chloride and iodide removal and oxidation[6,12] and bacterial and virus removal and inactivation.[9] Thus, CNT networks have potential to yield three-dimensional electrode structures that can be utilized for advanced water treatment. However, the dye oxidation was monitored by decolorization, which is not a good measure of oxidative strength. For example, the electrochemical filtration of methyl orange at an anode potential of 1.6 V resulted in a maximum of 17 electrons out of

Received: December 6, 2011
Accepted: February 7, 2012
Published: February 7, 2012

   dx.doi.org/10.1021/am2017267 | ACS Appl. Mater. Interfaces 2012, 4, 1478−1489

Table 1. Physical and Chemical Properties of Fresh and Electrolyzed Electrochemical Carbon Nanotube Networks

#	sample	phenol (mM)	Echem t	mass (mg)	d_{CNT} (nm)[a]	d_{pore} (nm)[a]	% CNT[b]	% Res[b]	% Poly[b]	burn peak T[b]	O/C[c]	S/C[c]	O/S[c]	B−N/C[c]	Na/S[c]
1	C-CNT	0	0	15.4	17.1 ± 6.6	104 ± 39	97.8	2.2	0.0	657, 637	0.026	0	0	n/a	
2	C-CNT	1	0	17.1	18.2 ± 7.4	96 ± 43	95.5	4.5	0.0	617, 604, 584, 551	0.030	0.003	10.7	n/a	3.15
3	C-CNT	0	5 h	41.7	18.9 ± 7.2	100 ± 42	68.4	31.6	0.0	541, 502	0.283	0.020	14.5	n/a	
4	C-CNT	0	5 h-wash	16.4	17.9 ± 8.4	106 ± 50	98.9	1.1	0.0	643, 625, 592	0.045	0	0	n/a	
5	C-CNT	0.2	5 h	52.3	34.2 ± 11.5	115 ± 55	23.3	27.3	40.4	524, 448, 391	0.309	0.070	4.5	n/a	2.50
6	C-CNT	1	5 h	46.8	29.9 ± 10.3	109 ± 52	38.3	17.9	43.7	563, 540, 485, 407	0.293	0.014	20.4	n/a	
7	C-CNT	1	5 h-wash	29.5	25.1 ± 8.1	114 ± 54	50.9	0.0	49.1	646, 627, 565, 462	0.075	0	0	n/a	
8	C-CNT	1	20 h	55.9	46.4 ± 12.5	140 ± 77	31.5	5.0	63.4	523, 438, 412, 327	0.289	0.019	15.3	n/a	2.70
9	B-CNT	0	0	15.6	18.6 ± 5.9	112 ± 46	99.0	1.0	0.0	737, 700	0.032	0	0	0.007	
10	B-CNT	0	5 h	33.8	20.1 ± 7.9	102 ± 41	77.5	22.5	0.0	554, 541	0.300	0.041	7.3	0.022	
11	B-CNT	0.2	5 h	50.2	29.5 ± 8.4	108 ± 48	31.4	25.6	43.0	570, 521, 426, 423	0.275	0.013	21.4	0.012	3.24
12	B-CNT	1	5 h	34.8	29.4 ± 7.7	117 ± 62	45.4	11.0	43.6	542, 507, 404, 373	0.272	0.009	30.3	0.004	
13	N-CNT	0	0	15.6	25.1 ± 13.6	99 ± 42	99.6	0.4	0.0	616, 560	0.033	0	0	0.013	
14	N-CNT	0	5 h	48.2	24.7 ± 8.7	123 ± 50	65.9	34.1	0.0	560, 518	0.224	0.016	13.7	0.020	
15	N-CNT	0.2	5 h	52.1	39.3 ± 13.6	118 ± 53	27.4	20.1	52.5	526, 493, 433, 365	0.561	0.062	9.1	0.018	2.98
16	N-CNT	1	5 h	47.1	33.4 ± 10.2	115 ± 53	31.0	17.6	51.4	553, 522, 454, 361	0.252	0.010	24.6	0.015	

[a]Determined by SEM. [b]Determined by TGA. [c]Determined by XPS.

a total of 80 electrons oxidized per dye molecule[6,13] and mass spectrometry indicated that azo bond breaking was the primary oxidation mechanism.[6] These results suggest that the refractory aromatic rings of methyl orange were still intact and thus more controlled experiments investigating the electrochemical filtration of simple aromatic molecules such as phenol are needed.

Along with more controlled experiments to investigate the oxidative strength of the electrochemical filter, the investigation of materials to rationally modify the oxidative strength of the network is also necessary. For example, there are a large number of CNTs of varying physical chemical properties such as diameter, chirality, and doping and the specific CNT selected will have significant affects on the network's electrochemical activity and oxidative strength. CNT doping with boron (B-CNT, p-type) or nitrogen (N-CNT, n-type) has been shown to effect the CNT electronic structure and in turn will likely also effect the CNT electrochemical activity. As compared to undoped carbon nanotubes (C-CNT), both the B-CNT and N-CNT have been observed to have a greater conductivity[14−16] and a higher specific capacitance[17,18] − two properties that are critical to electrochemical performance. The primary difference between the two dopants is their specific effect on the nanotube work function i.e, the distance from the material Fermi level to the vacuum level. The work function is 4.6 eV for C-CNT, 5.2 eV for B-CNT, and 3.9−4.4 eV for N-CNT[19,20] − the greater B-CNT work function suggests it may be the optimal material for driving oxidative processes. Due to their improved electronic properties as compared to undoped CNTs, both B- and N-doped CNTs have shown potential for electrochemical applications. The higher B-CNT work function makes it useful for sensing of electron-rich gases[21] and electroanalysis of biomolecules.[22] The lower N-CNT work function makes it useful as a reduction catalyst.[23] For example, N-CNTs have been observed to be more effective for oxygen reduction in fuel cells and reactive oxygen species production.[24] Thus, utilization of anodic B- and N-doped CNT networks may result in an increase in electrochemical filtration performance toward wastewater treatment.

Here, we utilize well purified and characterized undoped (C-CNT), boron-doped (B-CNT), and nitrogen-doped (N-CNT) carbon nanotube networks for the electrochemical filtration of an aromatic wastewater. Phenol (PhOH) is selected as the model aromatic pollutant as it is a produced on a large-scale, 10 million tons in 2008 as a precursor for resins and plasticizers,[25] and is a cocontaminant detected at 407 of the EPA's Superfund sites.[26] Phenol is also a good surrogate for the oxidatively recalcitrant aromatic moeties present in many micropollutants and natural organic matter. The electrochemical filters are challenged with 0.0, 0.2, and 1.0 mM phenol in 100 mM Na_2SO_4 electrolyte. The electrochemical oxidation efficiency is monitored by measurement of steady-state current and effluent total organic carbon (TOC) concentrations to determine apparent TOC removal efficiency and compare the efficacy of the three CNT networks. SEM, TGA, and XPS analysis of the CNT networks before and after electrochemical filtration yields insight into the electrode passivation mechanisms of electrochemical phenol polymerization and electrochemical electrolyte precipitation. Methodologies to reduce or eliminate passivation are discussed.

MATERIALS AND METHODS

Chemicals. Phenol (PhOH), hydrochloric acid (HCl; 36.5−38.0%), nitric acid (HNO_3; 69.8%), sulfuric acid (H_2SO_4; 95.0−98.0%), phosphoric acid (H_3PO_4;≥85.0%), ethyl alcohol (EtOH; ≥95.0%), dimethylsulfoxide (DMSO; ≥99.9%), potassium hydrogen phthalate (KHP), sodium sulfate (Na_2SO_4), sodium persulfate ($Na_2S_2O_8$), sodium bicarbonate ($NaHCO_3$), and sodium carbonate (Na_2CO_3) were purchased from Sigma-Aldrich (St. Louis, MO). All

chemicals were reagent grade except DMSO, which was spectrophotometric grade.

CNT Selection. The undoped multiwalled carbon nanotubes (C–CNT), nitrogen-doped multiwalled carbon nanotubes (N-CNT), and boron-doped multiwalled carbon nanotubes (B-CNT) were purchased from NanoTechLabs, Inc. (Yadkinville, NC). The CNTs were characterized in detail, Table 1, and have a diameter distribution in agreement with the manufacturer specifications. All CNTs were purified first by calcination and then with acid treatment prior to use and the purified CNTs will be referred to as "fresh" throughout the text.[27]

CNT Calcination. To remove any amorphous or other non-CNT carbon impurities, we first calcinated 1 g of as-received CNTs in a tube furnace by increasing from room temperature to 400 °C (300 °C for N-CNTs) for at a rate of 5 °C per min and holding for 60 min (Thermolyne, 21100).

CNT Acid Treatment. To remove the residual metal catalyst impurities, we placed 0.5 g of calcinated CNT into 0.5 L of conc. HCl acid and heated to 70 °C in a round-bottom flask with stirring and a condenser for at least 12 h. After heating, the sample was cooled to room temperature and vacuum filtered through a 5-μm PTFE membrane (Omnipore, Millipore) to collect the CNTs. The CNTs were then washed with Milli-Q deionized water (DI) until the filter effluent pH was neutral. The sample was then oven-dried at 100 °C before use.

Electrochemical CNT Filter Preparation. The CNT filters were produced by first dispersing the CNTs in DMSO at 0.5 mg/mL by probe sonication (Branson, Sonifier S450) for 15 min at an applied power of 400 W/L. Then, 30 mL of the CNTs in DMSO were vacuum filtered onto a 5-μm PTFE membrane (Millipore, Omnipore, JMWP), resulting in filter loadings of 1.5–1.6 mg/cm^2. The CNT filters were washed with 100 mL of EtOH, 100 mL of 1:1 DI-H_2O:EtOH, and 250 mL of DI-H_2O to remove DMSO. The prepared filter was loaded into a filtration casing modified for electrochemistry, as described in previous studies, see Figure S1 in the Suppporting Information.[6,9,12]

Solution and Electrochemistry. Sodium sulfate (Na_2SO_4; 100 mM) was utilized as the background electrolyte for all experiments. Phenol (PhOH) was used as the model aromatic pollutant as it is a high-volume industrial chemical and thus present in many industrial wastewaters and is also a common groundwater contaminant. The influent phenol–electrolyte solution was peristaltically pumped (Masterflex) through the electrochemical CNT filter and the steady-state electrochemistry was driven by a DC power supply (Agilent). The volumetric flow rate was 1.5 mL min^{-1}, which corresponds to a residence time in the electrochemical filter of ~1 s.[12] Bulk electrochemical filtration was first completed at a number of applied voltages over the range of 0.5 to 3.0 V. At each applied voltage, the effluent was collected for 30 min and the total current flowed was also collected for 30 min. Thus, every effluent and current measurement is a time average over this period. The effluent samples were then measured at least three times to ensure accuracy. Then, the applied voltage was held at a point that corresponded to 1.6 V anode potential for 3 to 5 h until the current reached a steady-state value. In this case, the total effluent flux and the total current flowed was collected between time points. Thus, every effluent measurement and current point in the time dependent plots is an average over time since the previous point. A number of parameters including effluent pH (Corning 345), effluent phenol concentration, total organic carbon (TOC) (Shimadzu TOC-VW), steady-state current, anodic potential, and back pressure were all recorded.

The apparent energy consumption (EC_{app}) for removing 1 kg of TOC was calculated with the following equation; EC_{app} (kWh (kg of TOC^{-1})) = $(UIt/3.6 \times 10^6)/(tJ\Delta TOC_{app})$, where U and I are applied voltage and steady-state current, respectively, t is reaction time, J is flow rate, and ΔTOC_{app} is the apparent TOC removal. The apparent mineralization current efficiency (MCE_{app}) was calculated with the following equation; $MCE_{app}(\%) = (\Delta TOC_{app}/\Delta TOC_{theor}) \times 100$, where ΔTOC_{theor} is theoretical TOC removal assuming all anodic current goes toward this process and is calculated using the following equation: ΔTOC_{theor} (mgC L^{-1}) = $((It/n_eF)n_cM)/(Vt)$, where F is Faraday's constant, F = 96485 C mol^{-1}, n_e = 28, the number of electrons removed during phenol mineralization, n_c = 6, the phenol carbon number, and M = 12 g mol^{-1}, carbon's atomic weight.

The CNT networks were also characterized using electrochemical methods (CHI Inc., CHI604D) such as double-layer capacitance and electrochemical impedance spectroscopy. The prepared CNT network was used as the working electrode, a stainless steel cathode was used as the counter electrode, and 1 M Ag/AgCl was used as the reference electrode in a flow cell configuration. Aqueous conditions were the same as bulk electrolysis.

TOC Analysis. The total organic carbon (TOC) analyses were completed on a Shimadzu TOC-VW analyzer equipped with a UV/thermal persulfate oxidizer. The TOC was calibrated over the concentration range of 1 to 100 mgC L^{-1} using a 6-point calibration curve with potassium terephtalate as a carbon source. Every sample was analyzed at least three times.

SEM Analysis. Scanning electron microscopy was completed in Harvard's Center for Nanoscale Systems on a Zeiss FESEM Supra55VP. Micrographs were analyzed with ImageJ software to determine apparent CNT diameter and aerial pore diameter, which is the distance between CNTs. Measurements were the average of at least 100 measurements from at least 2 network images. The SEM images at 50 kX and 100 kX for all CNT networks can be found in Figure S2 in the Supporting Information.

TGA Analysis. Thermogravimetric analysis was completed in Harvard's Material Research Science and Engineering Center on a Q5000-IR Thermogravimetric Analyzer (TA Instruments). Samples were heated from room temperature to 150 at 10 °C min^{-1}, held at this temperature for 30 min, then heated to 1000 at 10 C° min^{-1}, and held at this temperature for 30 min. A second run was completed immediately after the first and used as a background. The % residual catalyst was determined using the initial mass and mass remaining after a complete thermal cycle. The % polymer was determined by multiple Gaussian peak fitting to the dTG curve assuming the two highest temperature burn peaks were CNTs and using the areas to determine percent weight. The TGA and dTG plots with peak fittings can be found in Figure S3 in the Supporting Information for all CNT networks.

XPS Analysis. X-ray photoelectron spectroscopy was completed on an ESCA SSX-100 in Harvard's Center for Nanoscale Systems. For all samples, survey spectrum (0–1000 eV), C-1s (274–294 eV), O-1s (522–542 eV), and S-2p3 (155–175 eV) scans were completed. For the B-CNT samples, a B-1s (181–201 eV) scan was also completed. For the N-CNT samples, an N-1s (390–410 eV) scan was also completed. For a few samples, a Na-1s scan (54–74 eV) was completed for confirmation of salt precipitation. Data were analyzed using CasaXPS and ratios of integrated peak areas for the individual elements were used to determine the surficial carbon nanotube elemental ratios. The XPS spectra with peak fittings can be found in Figure S4 in the Supporting Information for all CNT networks.

RESULTS AND DISCUSSION

Characterization of Doped CNT Networks. The three carbon nanotube (CNT) samples examined in this study; undoped (C-CNT), boron-doped (B-CNT), and nitrogen-doped (N-CNT) were purchased from NanoTechLabs. The three CNT samples were formed into thin film networks by vacuum filtration of a recently ultrasonicated DMSO suspension. The CNT networks were then characterized by thermogravimetric analysis (TGA), scanning electron microscopy (SEM), and X-ray photoelectron spectroscopy (XPS) as presented in Figure 1, Table 1. The surficial O/C ratio as determined by XPS for all three CNT samples is similar falling between 0.025 to 0.035 and the surficial B- and N-doping as determined by XPS is around 1% (Table 1). The TGA burn temperatures in Figure 1A indicates that the B-CNT are the most oxidatively stable CNT followed by C-CNT and then N-CNT, in agreement with previous reports that B-doped CNTs

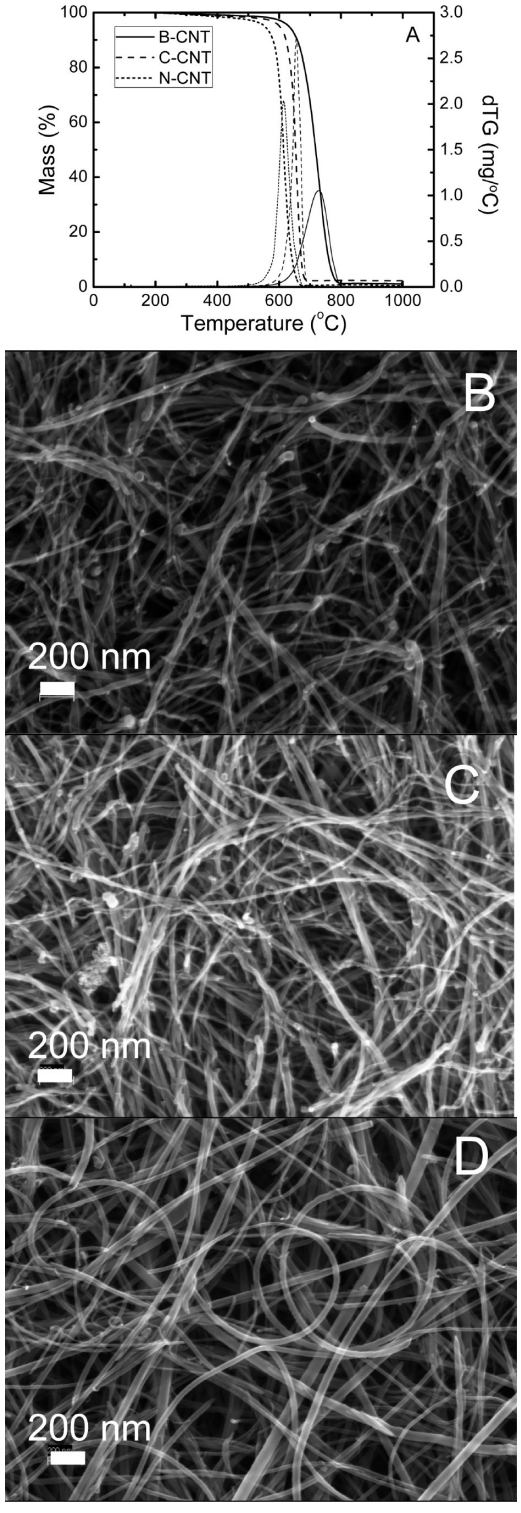

Figure 1. Scanning electron micrographs and thermogravimetric analysis of fresh CNT networks. (A) Mass percent and dTG (peaks) in mg $°C^{-1}$ as a function of temperature for fresh B-CNT (solid), C-CNT (dashed), and N-CNT (short dash) networks. (B–D) Scanning electron micrographs of the B-CNT, C-CNT, and N-CNT, respectively.

have increased graphitization.[28] The TGA also indicated that the three CNT samples were at least 97.5% CNT and the doped CNTs were ≥99.0% CNT. SEM of the C-CNT, B-CNT, and N-CNT networks are presented in Figure 1B–D, respectively. The B-CNT and C-CNT have a similar average diameter of 17–19 nm. In contrast, the N-CNTs are larger with an average diameter of ~25 nm. The pore size distribution of the three networks is similar with an average pore diameter of around 105 nm and a standard deviation of ~45 nm. A primary difference between the three materials is their previously reported work functions[19,20] that correspond to Fermi level redox potentials (vs NHE) of −0.1 V for the N-CNT, 0.1 V for the C-CNT, and 0.8 V for B-CNT.

Electrochemical Filtration Performance Toward Phenol Removal. The electrochemical filtration performance of the CNT networks was evaluated at a liquid flow rate of J = 1.5 mL min^{-1} and an influent electrolyte concentration of 100 mM Na_2SO_4. The filter was challenged with phenol (PhOH), a model aromatic wastewater, at two influent concentrations of 0.2 and 1.0 mM as presented in Figure 2. The data for the control experiment with no phenol can be found in Figure S5 in the Supporting Information. At 0.2 and 1.0 mM influent phenol concentrations, the CNT surface will be immediately saturated with a monolayer of phenol due to the strong[29,30] and fast[12] adsorption of aromatics to the CNTs. The steady-state current (mA) of the 0.2 mM PhOH and the 1.0 mM PhOH in 100 mM Na_2SO_4 as a function of voltage, 0.0 to 3.0 V, and time, 0 to 280 min, is presented in Figure 2A,D, respectively. For all three CNT networks and at both influent phenol concentrations, the current becomes >0 mA once the applied voltage is increased to >1.5 V and increases monotonically with increasing voltage. Similarly, the anode potential also increases monotonically and linearly with increasing applied voltage, Figure 3A (0.2 mM PhOH) and Figure 3D (1.0 mM PhOH), with roughly 50% of the applied voltage going toward the anode potential. The aqueous electrochemical phenol filtration was continued at an anode potential of 1.6 V, corresponding to an applied voltage of 3.0–3.3 V as this was the highest voltage at which the system was stable for an extended period, >6 h. At an anode potential of 1.6 V and at both influent phenol concentrations, the current is observed to decrease for the first 2 to 3 h until a steady-state current value is achieved. The decreasing current with time indicates the CNT electrodes are partially passivated. The B-CNT network is the most resistant toward electrochemical passivation, i.e., the B-CNT network has the smallest decrease in current during electrolysis at −5 mA as compared to −13 mA for the C-CNT network and −19 mA for the N-CNT network. A similar trend in current with time as a function of doping is observed when the influent phenol is 1.0 mM. The B-CNT network has the smallest decrease in current with time at −6 mA, followed by the C-CNT at −18 mA, and once again the N-CNT has the largest decrease in current at −20 mA. The B-CNT network resistance toward electrooxidative passivation suggests it may be the optimal CNT for anodic processes such as wastewater treatment.

The effluent total organic carbon (TOC) concentration is plotted versus voltage and time in panels B and E Figure 2 for influent phenol TOC concentrations of 15 mgC L^{-1} and 72 mgC L^{-1}, respectively. When the influent phenol is 15 mgC L^{-1}, the effluent TOC trend is similar for B-CNT and C-CNT with the TOC decreasing with increasing voltage until ~2 V when $[TOC]_{ef}$ = 9–11 mgC L^{-1} and then decreasing with time for the first 2 h of electrolysis until a steady-state effluent TOC concentration of 7–8 mgC L^{-1}, 50% of influent TOC, is achieved. In contrast, over the applied voltage range of 2.0–3.0 V, the N-CNT effluent TOC decreases much lower than the B-CNT and C–CNT and in the range of 2–6 mgC L^{-1}.

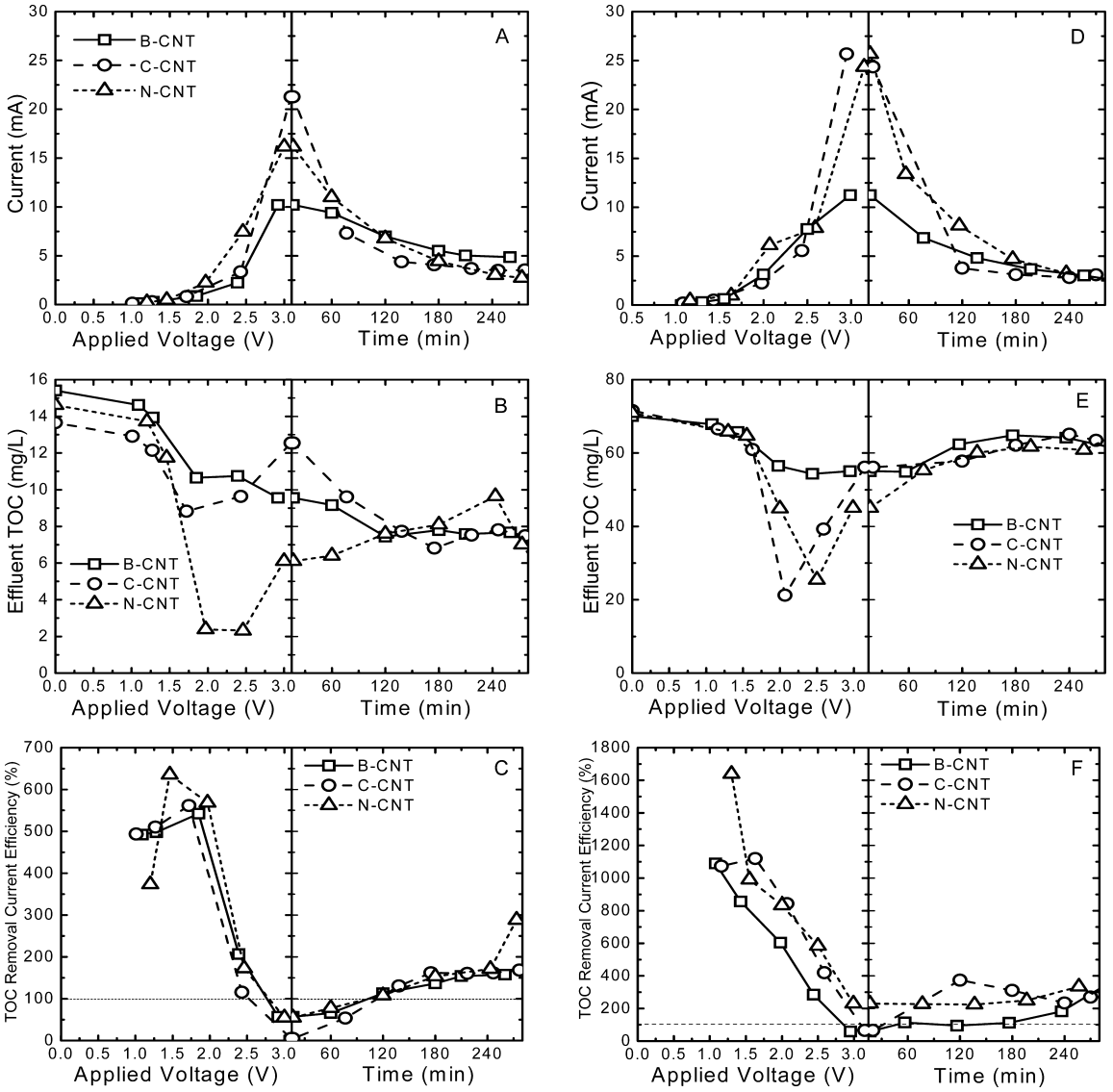

Figure 2. Electrochemical filtration of phenol as a function of CNT doping, applied voltage, and time. In all cases, the applied voltage was increased until the anode potential reached 1.6 V vs SCE as described in the left half of the plots and then the electrolysis was continued for another 5 h as described in the right-hand of the plots. Electrochemical conditions were J = 1.5 mL min^{-1} and [Na_2SO_4] = 100 mM for B-CNT (squares-solid line), C-CNT (circles-dashed line) and N-CNT (triangles-short dash line). The influent phenol concentration was 0.2 mM for A–C and 1.0 mM for D–F. (A, D) Current (mA), (B, E) effluent total organic carbon (mgC/L), and (C, F) TOC removal current efficiency (%) versus applied voltage (V) and time (min). The dashed horizontal lines in C and F represent 100% efficiency.

However, after 2 h of electrolysis, the N-CNT effluent TOC achieves a steady-state extent of oxidation similar to the B-CNT and C–CNT networks at Δ[PhOH] = 7–8 mgC L^{-1}. The steady-state extent of oxidation when the influent phenol is 72 mgC L^{-1}, Figure 2E, is also in this range, Δ[PhOH] = 7–9 mgC L^{-1}, indicating that even at the lower influent concentration, the phenol oxidation process is saturated. The large decrease in effluent TOC between 2.0 and 3.0 V is again observed when the influent phenol is 72 mgC L^{-1}, but in this case for both the C-CNT and N-CNT networks. At an applied voltage of 2.0 V, where the strong decrease in effluent TOC is initially observed, the anode potential for all three networks is in the range of 0.8–0.9 V, Figure 3A, D. This anode potential range is near the reported one-electron oxidation potential of phenol at 0.82 V that would yield reactive phenolic radicals.[31] Thus, the strong decrease in effluent TOC over the applied voltage range of 2.0 to 3.0 V is likely due to electrochemical polymer formation via phenolic radical chain reactions.[32] Further discussion of electrochemical phenol oxidation products and their subsequent chemistry is warranted.

The electrochemical oxidation mechanism of phenol has been well studied and follows the general reaction of eq 1 where n is the number of electrons oxidized from phenol with n = 28 for complete mineralization.[33–35]

$$C_6H_5OH + nh^+ \rightarrow \text{products} \quad (1)$$

The one electron oxidation of phenol will produce the phenoxy radical, eq 2, which can either undergo further oxidation to a hydroquinone, eq 3, or react with another phenol molecule, eq 4, or phenol oxidation product and initiate the chain polymerization process. The subsequent one electron oxidation potential of the hydroquinone product of eq 3 is lesser than phenol, and thus will occur simultaneously, eq 5. The

dx.doi.org/10.1021/am2017267 | ACS Appl. Mater. Interfaces 2012, 4, 1478–1489

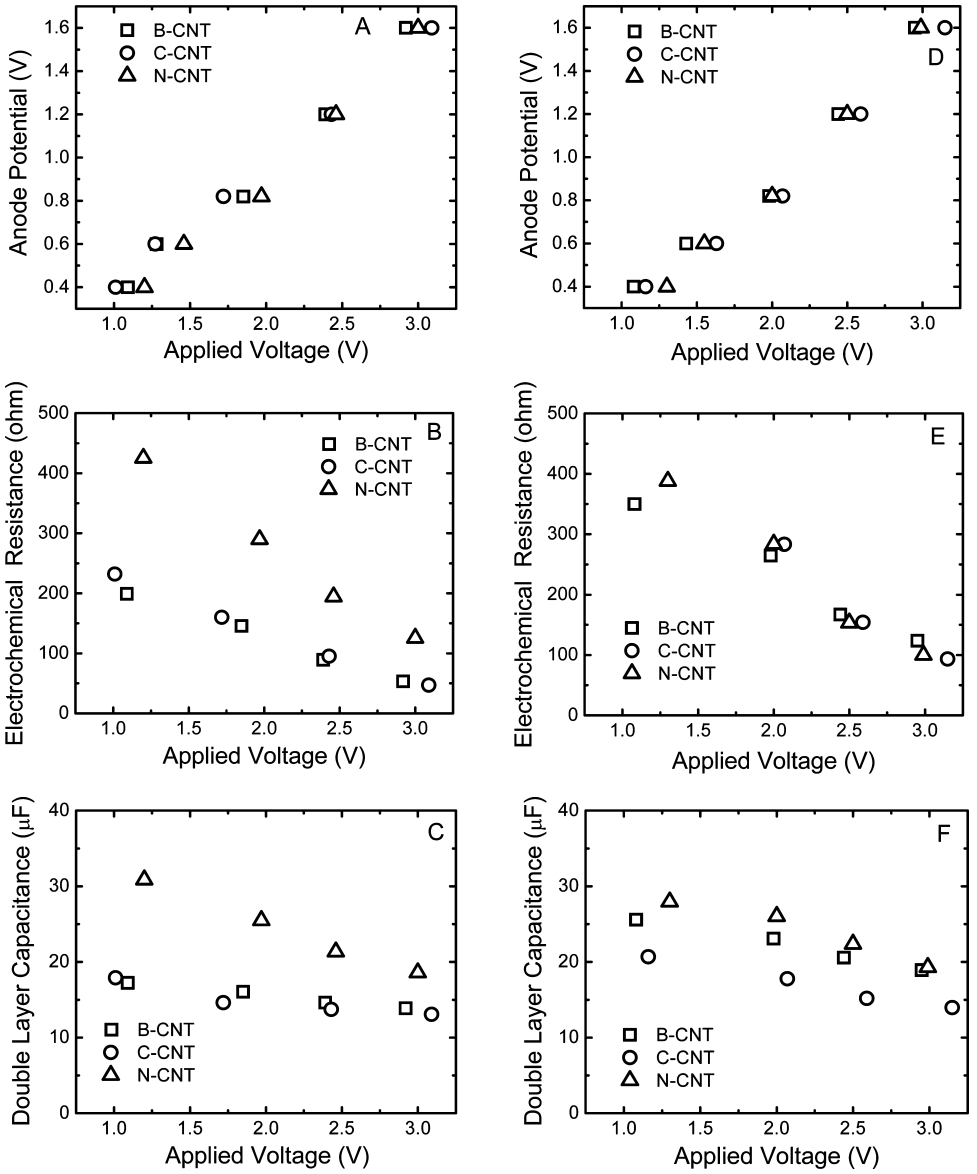

Figure 3. Electrochemical characteristics of the CNT network during electrochemical filtration of phenol as a function of CNT doping and applied voltage. electrochemical conditions were J = 1.5 mL min^{-1} and [Na_2SO_4] = 100 mM for B-CNT (squares), C-CNT (circles), and N-CNT (triangles). The influent phenol concentration was 0.2 mM for A–C and 1.0 mM for D–F. (A, D) Anode potential (V) vs applied potential (V), (B, E) electrochemical resistance (ohm) vs applied voltage (V), and (C, F) double layer capacitance (μF) vs applied voltage (V).

subsequent hydroquinone radical may also participate in the chain polymerization process, eq 6.

$$C_6H_5OH + h^+ \rightarrow C_6H_5O\cdot \quad (2)$$

$$C_6H_5O\cdot + h^+ + H_2O \rightarrow C_6H_4(OH)_2 + H^+ \quad (3)$$

$$C_6H_5O\cdot + C_6H_5OH \rightarrow C_6H_5OC_6H_4O\cdot \quad (4)$$

$$C_6H_4(OH)_2 + h^+ \rightarrow C_6H_4(OH)O\cdot \quad (5)$$

$$C_6H_4(OH)O\cdot + C_6H_5OH \rightarrow C_6H_4(OH)OC_6H_4O\cdot \quad (6)$$

The three primary classes of stable phenol oxidation products are listed here in order of increasing extent of oxidation; the hydro- and benzo- quinones and corresponding phenolic radicals that can polymerize, small organic acids such as maleate and bioxalate, and the complete mineralization product – carbon dioxide. The one-electron redox potential at pH 7 of phenol is 0.8 V, of the quinone family is 0.0–0.8 V, and of small organic acids is 1.0–2.0 V.[31] Thus, once the anode potential is increased above 0.8 V, the spontaneous formation of a wide range of phenol and quinone i.e., phenols, based radicals will occur and these radicals can react with phenol or another quinone, eq 4 and 6, to initiate a chain polymerization process. This phenols polymerization process is likely responsible for the strong decrease in effluent TOC once the applied voltage has been increased over 2.0 V corresponding to an anode potential of 0.8–0.9 V for the N-CNT network at 0.2 mM phenol, Figure 2A, and for the N-CNT and C-CNT network at 1.0 mM phenol, Figure 2D. The extent of phenol oxidation in terms of n electrons removed per molecule is expected to increase with both increasing anode potential and increasing material work function i.e., Fermi level redox potential. Thus, although we observe similar TOC removal for all three CNT networks, the extent of phenol oxidation may be dissimilar.

dx.doi.org/10.1021/am2017267 | ACS Appl. Mater. Interfaces 2012, 4, 1478–1489

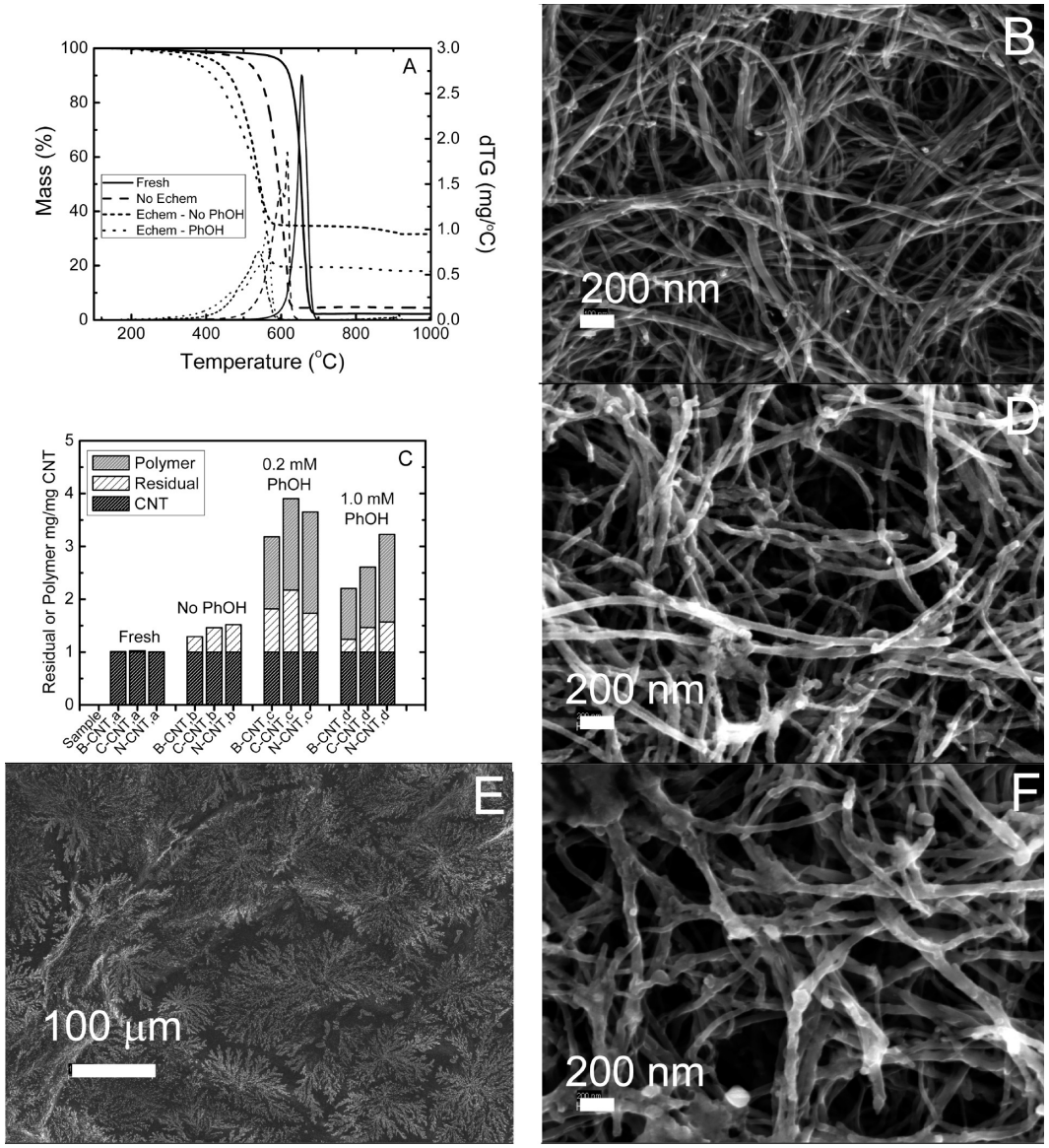

Figure 4. Evidence for electrochemical phenol polymerization and electrolyte precipitation. Electrochemical C-CNT filtration conditions were J = 1.5 mL min^{-1}, [Na_2SO_4] = 100 mM, t = 5 h, and 3 V. (A) TGA mass percent and dTG (peaks) of a fresh C-CNT network (solid), C-CNT network after filtration of 1 mM phenol in the absence of potential (dashed), C-NT network after electrochemical filtration (short dash), and C-CNT network after electrochemical filtration of 1 mM phenol (dot). (B) SEM of fresh C-CNT network, (C) percent CNT, residual, and polymer versus CNT network, (D) SEM after electrochemical filtration of 1 mM phenol, (E) SEM of N-CNT network after electrochemical filtration of 1 mM phenol, and (F) SEM of electrochemical filtration of 1 mM phenol for 20 h.

Thus, the resulting increase in effluent phenol at applied voltages >2.5 V would then indicate a shift to more oxidized products that cannot polymerize. Similarly, the absence of a strong decrease in phenol concentration for the B-CNT network at both 0.2 and 1.0 mM would indicate that the B-CNT's greater work function results in a greater extent of phenol oxidation to yield a greater fraction of products that cannot polymerize.

The steady-state current and TOC removal from the influent solution are used to calculate the apparent TOC removal current efficiency assuming that any TOC loss is representative of electrochemical phenol combustion to carbon dioxide (n = 28 for eq 1), Figure 2C and 2F. It is of note that for all three CNT networks at an influent phenol concentration of 0.2 mM, the current efficiency is >100% when the applied voltage is <2.5 V and when $t \geq 120$ min. For the B-CNT and C-CNT networks, the current efficiency never drops below 50%. Even greater TOC removal current efficiencies, 60 to 1,200%, are observed when the influent phenol concentration is 1 mM, Figure 2F. The >100% current efficiency indicates that the assumption of complete electrochemical combustion to CO_2 is invalid and as stated earlier, electrochemical phenol polymerization is active. Although the influent phenol is not completely oxidized, the electrochemical polymerization process is energy efficient toward phenol removal e.g., when the applied voltage is ≤2.5 V and $[PhOH]_{in}$ = 0.2 mM the energy required is <25 kWh (kg TOC)$^{-1}$ and when $[PhOH]_{in}$ = 1.0 mM the required energy is <10 kWh (kg TOC)$^{-1}$.[4] The extent of electrochemical phenol removal is also notable considering the influent aqueous solution only spends ~1 s within the electrochemical CNT network.[12]

The three CNT network's electrochemical filtration performance toward aqueous phenol removal is relatively similar likely a result of the high influent phenol concentration that saturates the surface-limited electrochemical process. The B-CNT network showed the most promise as an anodic substrate because it displayed the lowest extent of electrochemical passivation and the N-CNT showed the most promise for electrochemical phenol polymerization. The extent of electrochemical passivation is observed to be inversely proportional to the CNT work function.[19,20] This suggests that although the performance of the three materials toward phenol removal is similar, the B-CNT may be able to oxidize the individual phenol molecules to a greater extent i.e., the *n* in eq 1 is greatest for the B-CNT and lowest for the N-CNT. The greater extent of oxidation would bypass the formation of polymerizing organic free radicals.[34] To gain further insight into these differences, the anode potential, electrochemical impedance, and double-layer capacitance were measured as a function of applied voltage and influent phenol concentration as presented in Figure 3. The observed anode potentials (Figure 3A, D) for the three CNT samples increased linearly with applied voltage and are independent of both material and phenol concentration. The electrochemical resistance (Figures 3B, E) measures the resistance to electron transfer and electropolymerization would be expected to increase resistance due to CNT coating by an insulating polymer. In all cases, the electrochemical resistance is observed to linearly decrease with increasing applied voltage as expected since electron transfer rates increase linearly with increasing potential. At an influent phenol concentration of 0.2 mM, the resistance is greater for the N-CNT by 75 to 150 ohm at all applied voltages as compared to the C-CNT and B-CNT. This is in agreement with the effluent TOC results presented in Figure 2B, where a large decrease in effluent TOC, an indicator of highly active electropolymerization, is observed only for the N-CNT network. At the higher influent phenol concentration of 1.0 mM, the electrochemical resistance for the three CNT networks converges suggesting that polymerization process is enhanced as expected by eq 4, but also has a saturation limit since the N-CNT resistance does not increase from 0.2 to 1.0 mM phenol.

The double-layer capacitance (Figure 3C, F) is a measure of an electrode's ability to store charge at a specific voltage. In all cases, the capacitance is observed to decrease linearly with increasing applied voltage as expected since Faradaic electron transfer, which will reduce electrode charge, increases with increasing potential. Similar to the resistance results at 0.2 mM influent phenol, the N-CNT capacitance values were greater at all voltages as compared to the B-CNT and C-CNT values, which were similar. The greater N-CNT capacitance is in agreement with previous reports and indicates a larger number of electrochemically active sites[18] consistent with the greater electropolymerization TOC removal by the N-CNT network. The voltage dependent capacitance for both the B-CNT and C-CNT converges with the N-CNT values when the phenol concentration is increased to 1.0 mM, similar to the resistance results. This again indicates that at the higher influent phenol concentration, the electrochemical process is saturated. In all cases where phenol was used in the influent solution, the capacitance is increased over the control with no phenol, see Figure S5D in the Supporting Information. This suggests that the produced polymer increases the number of capacitance sites. In summary, the capacitance, resistance, current, and TOC data all indicate that electropolymerization of phenols, i.e., phenol and/or the quinone intermediates, is occurring and results in the passivation of the electrode. And the extent of passivation is inversely correlated to the work function of the material with the B-CNT displaying the least passivation. Thus, in the following sections, a number of CNT network material analyses both before and after electrolysis will be completed to examine the passivating polymers in greater detail.

Evidence for Electrochemical Phenol Polymerization and Electrolyte Precipitation. The observations of decreasing current with time and >100% TOC removal current efficiencies are both indicative of electrochemical polymer formation on the CNT anode resulting in passivation. The polymer formation is also supported by large increases in CNT network weight postelectrolysis, Table 1. To further investigate the mechanism of polymer formation, we completed TGA, SEM, and XPS on all of the electrolyzed CNT samples, Table 1. Upon inspection of the TGA data, it was not only confirmed that electrochemical polymer formation was active but that electrochemical electrolyte or salt precipitation was also active, panels A and C in Figure 4. In Figure 4A, the mass percent and dTG versus T was plotted for a fresh C−CNT network, a C-CNT network that filtered phenol in the absence of electrochemistry, an electrolyzed C-CNT network with 0.0 mM influent phenol, and an electrolyzed C-CNT network with 1.0 mM influent phenol. For both electrolyzed CNT networks, the TGA results showed that the residual mass percent increased to ≥15% as compared to ∼2% for the fresh CNT network and ∼4% for the nonelectrolyzed C-CNT network, indicating electrochemically mediated electrolyte precipitation. For the C−CNT networks electrolyzed with phenol, a large low T burn shoulder appears in the dTG curve due to polymer formation. Gaussian multipeak fitting of the dTG curve was used to calculate the percent polymer of the electrolyzed samples.

The analyzed TGA data for the majority of the electrolyzed CNT samples are presented in Figure 4C with the precipitate and polymer mass normalized to the CNT mass. Electrochemically mediated precipitate formation was observed for all electrolyzed CNT networks and polymer formation was observed for all CNT networks electrolyzed in the presence of phenol. The electrochemically mediated polymer and precipitate formation is confirmed by aerial SEM images of the electrolyzed CNT networks presented in Figure 4B, D−F. The B, D, and F images are of a fresh C-CNT network, a C-CNT network electrolyzed with phenol for 5 h, and a C-CNT network electrolyzed with phenol for 20 h. The apparent CNT diameter is visibly observed to grow with time during phenol electrolysis and CNT diameter growth is also observed for the N-CNT and B-CNT networks, Table 1. This growth is attributed to electrochemical polymer formation and is due to partial phenol oxidation resulting in the formation of phenol-based organic radicals that take part in a free-radical chain polymerization process, eqs 4 and 6.[35] Visual confirmation of electrochemical precipitate formation is presented in Figure 4E for an N-CNT sample electrolyzed for 5 h. Salt crystals have obviously coated the N-CNT network surface. The electrochemical precipitation may be driven by the increased ion activity within the CNT electrical double layer of the electrolyte or electrochemically produced salts. An alternative precipitation mechanism is the electrochemical oxidation of sulfate to persulfate[36] whose sodium salt is significantly less soluble in

water at 20 °C than sodium sulfate i.e., 23 mM for $Na_2S_2O_8$ versus 900 mM for Na_2SO_4.

The B-CNT network as compared to the C-CNT and N-CNT networks is observed to have the lowest extent of electrochemical polymer and precipitate formation under all influent aqueous conditions, Figure 4C. The extent of both electrochemical polymer and precipitate formation increases with decreasing CNT work function. Both the polymer and precipitate will coat the electrochemically active surface with an insulating material and passivate the electrode. Thus, the polymer and precipitate formation results indicate that the B-CNT is the most resistant to electrochemical passivation in agreement with chronoamperometry results, Figure 2A, as well as the higher reported B-CNT work function and hole transport properties.[19,20] The N-CNT network is observed to have the greatest extent of polymer and precipitate formation, in line with the increased TOC removal via polymer formation, Figure 2B, and increased double layer capacitance, Figure 3.[18]

Electrochemical Salt Formation versus CNT Oxidation. The electrolyzed C-CNTs thermogravimetric burn temperature is decreased from near 650 °C for the fresh C-CNT network to between 500 and 550 °C for the electrolyzed C-CNT network and a similar result is observed for the electrolyzed N-CNT and B-CNT networks, Figure 4A and Table 1. The reduction in burn temperature may be caused by electrochemical oxidation of the CNTs introducing more easily combustible sp^3 defects into the normally sp^2-bonded CNT surface.[37] Another possible cause could be CNT cocombustion with the precipitate or polymer due to thermal production of oxidizing radicals, e.g., the thermolysis of persulfate to produce the strongly oxidizing sulfate radical.[38] To discern between these two possibilities, an attempt was made to wash the precipitate and/or polymer from the electrolyzed CNT network with an acidic ethanol−water solution. The TGA results of the C-CNT networks electrolyzed in the absence and presence of phenol and the same samples after washing are presented in Figure 5A,B. The washed C-CNT networks have nearly all of the precipitate removed, i.e., <1.2% residual mass in both samples, and have TGA burn temperatures near that of a fresh C−CNT network. Only a small fraction of the polymer was removed by the wash indicating the decrease in burn T in the electrolyzed networks is primarily due to the precipitate catalyzed CNT combustion. For example, if sodium persulfate precipitated as previously hypothesized, the thermal dissociation of persulfate to two strongly oxidizing sulfate radicals ($S_2O_8^{2-} + \Delta \rightarrow 2\ SO_4\cdot^-$) would reduce the burn temperature of the CNTs.

To gain further insight into the specific precipitate responsible for the decreased burn *T*, the O/C, S/C, and S/O ratios determined from the XPS spectra of the electrolyzed and electrolyzed-then-washed C-CNT networks are presented in Figure 5C. The large O/C ratio of the electrolyzed CNT networks indicates a highly oxygenated precipitate. The nonzero S/C ratio in these samples indicates that sodium sulfate or persulfate may be responsible for the observed O/C ratios. However, the S/O ratio for both salts is 0.25, well above the observed values of 0.07 and 0.04, indicating another salt was also present. One possibility is sodium carbonate as there is evidence for Na_2CO_3 in the TGA of the electrolyzed samples, Figure 5A, where mass loss is observed between 800 and 900 °C.[39] The washed samples have no sulfur signal and a reduced O/C ratio, indicating that the XPS spectrum of the electrolyzed CNT networks is representative of the precipitate. The O/C

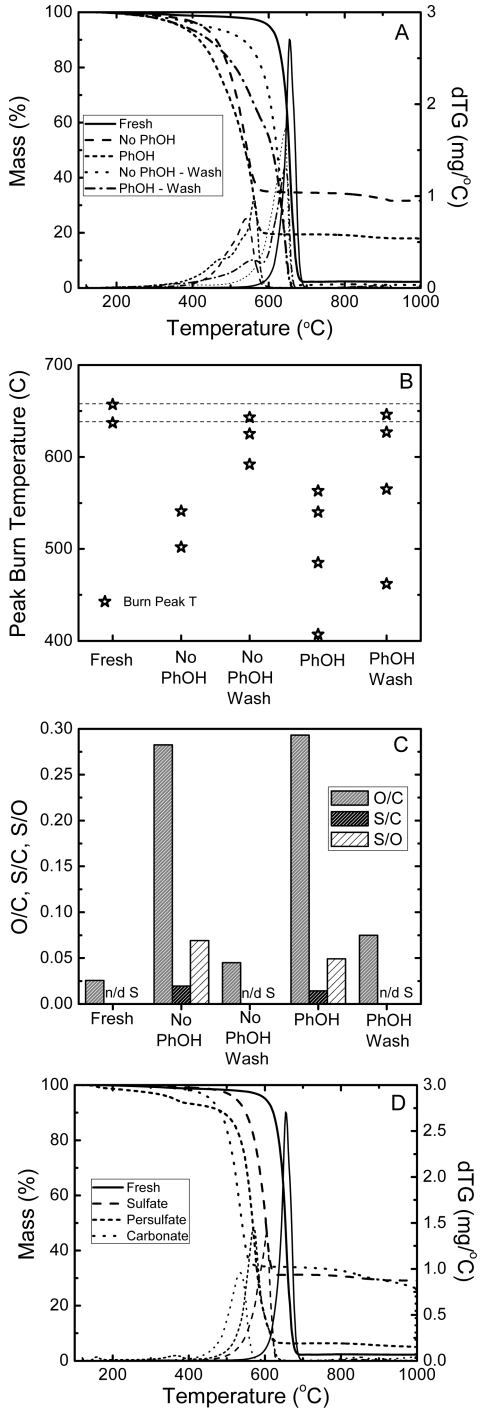

Figure 5. CNT oxidation versus electrolyte precipitation. Electrochemical C-CNT filtration conditions were J = 1.5 mL min^{-1}, [Na_2SO_4] = 100 mM, t = 5 h, and 3 V. (A) C-CNT network thermogravimetric analysis percent mass versus temperature and dTG (peaks) plots for fresh (1, solid), electrochemical filtration (3, dash), electrochemical filtration with 1 mM phenol (6, short dash), electrochemical filtration sample washed with acidic water−ethanol mixture (4, dot), and electrochemical filtration with 1 mM phenol sample washed with acidic water−ethanol mixture (7, dash dot). (B) Burn peak temperature of samples from A. (C) XPS O/C, S/C, and S/O ratios of samples from A. (D) C−CNT network thermogravimetric analysis percent mass versus temperature (solid) and dTG (dash) plots for fresh network (black) and networks mixed with 20% w/w of sodium sulfate (red), potassium persulfate (green), and sodium carbonate (blue).

dx.doi.org/10.1021/am2017267 | ACS Appl. Mater. Interfaces 2012, 4, 1478−1489

ratio is slightly greater in the electrolyzed-then-washed CNT networks, 0.045 to 0.075, as compared to the fresh C-CNT networks, 0.026. The increased O/C ratio could be due to electrochemical CNT oxidation and/or electrochemical polymer formation since only a small fraction of the polymer is removed during the wash step. To determine which is more likely, an estimation of the theoretical O/C ratio of the electrolyzed with phenol then washed C−CNT network will be made assuming that the polymer has a similar O/C ratio to the phenol monomer of 0.17. The fresh C-CNT network has an O/C ratio of 0.025 and the electrolyzed with phenol then washed C-CNT network is 50% polymer and 50% CNT, thus the estimated O/C ratio would be 0.095, which is slightly greater than measured O/C ratio of 0.075 indicating that polymer formation is primarily responsible for the O/C ratio increase. However, electrochemical CNT oxidation cannot be ruled out completely because the O/C ratio does increase slightly to 0.045 in the network electrolyzed in the absence of phenol.

To further evaluate whether the presence of the precipitates would reduce the CNT burn temperature, they were individually mixed with fresh CNTs by ultrasonication, dried, and thermogravimetrically analyzed, Figure 5D. In all cases, the CNT burn T decreased with the extent of decrease following the order carbonate (525 °C) > persulfate (550 °C) > sulfate (600 °C). The carbonate and persulfate induced burn Ts are quite similar to the electrolyzed CNT burn Ts suggesting these are the major electrochemical precipitates. Based on concentrations, the precipitate is most likely persulfate because the influent sulfate is 100 mM and the influent phenol is 1 or 0.2 mM. Finally, the decreased electrolyzed CNT network burn temperature is due to precipitate formation and not CNT oxidation.

Electrochemical Polymerization. During the electrooxidation of aqueous aromatics such as phenol, if the anode potential is below 2.3 V, then polymerization forming species such as polyphenol or polyoxyphenylene will occur.[33,35] Because these polymers are more insulating as compared to the anode, the electropolymer growth and coating will act to passivate the active electrode surface. Thus, it is of importance to investigate the electropolymerization process such that methods to prevent passivation and/or to regenerate the active electrode surface can be developed. In this study, the time-dependent electrolysis is completed at an anode potential of 1.6 V or 3.0−3.3 V as this is the highest voltage at which the system is stable for an extended period of time. Both electrode passivation, i.e., the current decrease over the first two hours of electrolysis in Figure 2, and polymer formation are observed, Figure 5. The extent of polymer formation is quantified here by TGA and SEM of the electrolyzed CNT samples, Table 1 and Figure 6. There are two TGA polymer burn peaks observed in all of the electrolyzed CNT networks. Both peaks occur at a lower temperature as compared to the CNT burn peaks and the higher T peak is always the major polymer peak. Assuming that similar to the CNTs, the polymer burn T of the electrolyzed then washed network is a more accurate representation of the material, then typical electropolymer burn Ts are ∼560 and 460 °C. The higher burn T of 560 °C is typical of species with a conjugated π-bonded structure indicating the sp^2-conjugation of the phenol monomer has been maintained,[40] in agreement with phenols precipitation. The percent polymer mass of the electrolyzed CNT samples was similar for B-CNT and C-CNT at 40−44% and was greater for the N-CNT sample at 51−53%. The percent polymer mass was independent of influent phenol

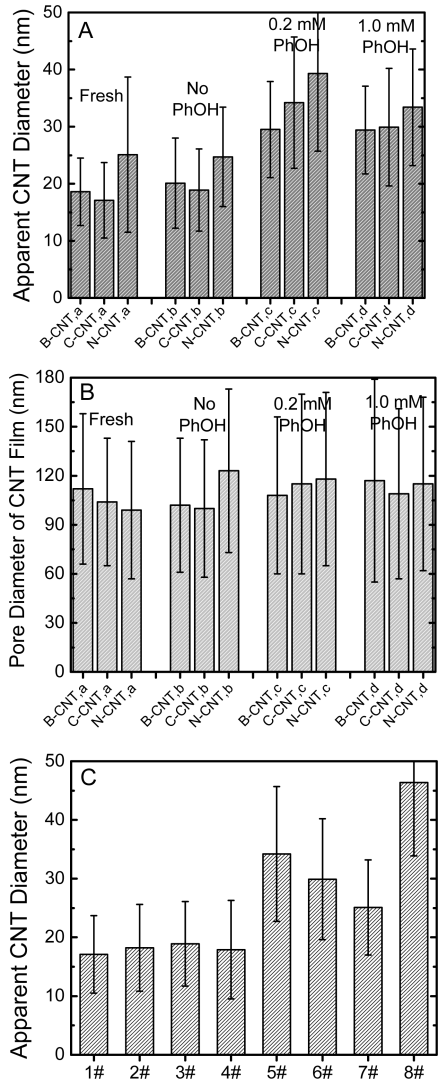

Figure 6. Electrochemical polymer growth. (A) SEM CNT diameter (nm) as a function of doping (B, C, N), electrochemistry (applied potential vs no applied potential), and phenol concentration (0, 0.1, 1.0 mM). (B) SEM CNT network pore diameter as a function of doping, electrochemistry, and phenol concentration. (C) SEM C−CNT diameter as a function of electrochemistry, phenol concentration, network washing and electrolysis time. The number label in the x-axis of part C corresponds to the sample no. from Table 1.

concentration likely due to the strong and fast adsorption of the aromatic phenol to the CNT surface[29,30] and resulting saturation of the surface-limited electrochemical process.

The apparent CNT diameter as determined by SEM for the fresh and electrolyzed CNT networks is presented in Figure 6a. The formation of polymer was only observed when phenol was present in the influent solution. If phenol was present, the apparent CNT diameter grew by 8 to 17 nm. However, even though the apparent CNT diameter grew by >50% as compared to the initial diameter, there was negligible effect on the average network pore size, Figure 6B. Insight into the polymer identity can be gained by calculating the polymer density (ρ_{poly}) from the TGA polymer mass (m_{poly}) and SEM polymer volume (V_{poly}) using the equation; $\rho_{poly} = m_{poly}/V_{poly} = (m_f\%_{poly} r_i)/(SSA_{CNT} m_i(r_f^2 - r_i^2))$ where m_i and m_f are the initial and final CNT network mass, $\%_{poly}$ is the percent polymer by TGA, r_i and r_f and the initial and final apparent CNT radius by

dx.doi.org/10.1021/am2017267 | ACS Appl. Mater. Interfaces 2012, 4, 1478−1489

SEM, and SSA_{CNT} is the specific surface area of the CNT.[12] The average polymer density for all of the electrolyzed networks is $\rho_{poly} = 1.05 \pm 0.04$ g cm^{-3}. The calculated polymer density is quite similar to the density, 1.1 g cm^{-3}, of polyphenylene ether and polyphenylene oxide, which are both plausible products of the electrochemical polymerization of phenol and in agreement with previous reports.[33−35]

The diameter for all of the C−CNT networks is presented in Figure 6C and the number label in the *x*-axis corresponds to sample number in Table 1. Again, only the apparent diameter of the electrolyzed CNT networks with phenol present, 5−8, grew by a large amount. The acidic ethanol−water wash of an electrolyzed CNT network, 7, was able to remove a fraction of the polymer reducing the diameter by ∼5 nm; however, the postwash diameter was still 6−7 nm greater than the initial diameter. Finally, it was observed that after extended electrolysis of 20 h, 8, the apparent CNT diameter grew even further to nearly 3-fold greater, ∼46 nm, the initial CNT diameter, ∼17 nm, indicating that the polymer coating did not completely passivate the anodic CNT network. Future studies will investigate in situ methods for CNT electrode regeneration such as increasing anode potentials to >2.3 V[34] and chemical washing with nonaqueous solvent similar to the acidic ethanol−water removal of the precipitate.

CONCLUSION

The efficacy of undoped (C-CNT), boron-doped (B-CNT), and nitrogen-doped (N-CNT) networks toward the electrochemical filtration treatment of aromatic wastewaters using phenol as a model aromatic pollutant was examined here. In terms of steady-state total organic carbon removal, all three CNT networks were able to remove a similar amount of the influent phenol at an anode potential of 1.6 V under steady-state conditions, ∼ 7 to 8 mgC L^{-1} or ∼50% of the 0.2 mM influent phenol. The similar performance is likely due to saturation of the electrochemical process at high influent phenol concentrations. All three CNT networks were passivated to various extents during the electrochemical process and the extent of passivation was inversely correlated to the CNT work function. Three observations have led us to conclude the B-CNT network was the most resistant to passivation; the B-CNT network had the least reduction of current during extended electrolysis at 3.0 V applied voltage, the effluent TOC of the B-CNT network did not decrease sharply at 2.0 V—a representative sign of polymerization, and under all conditions the extent of polymer and precipitate formation was the least with the B-CNT network. The passivation of the anodic CNT networks was determined to occur through electrochemical formation of insulating precipitate and polymer coatings on the surface of the CNTs. SEM and TGA analysis of the electrolyzed CNT networks showed that the B-CNT network had the lowest extent of electrochemical polymer and precipitate formation. The predominant electrochemical precipitate was determined to likely be sodium persulfate or carbonate by TGA and XPS and could be removed with a simple acidic water−ethanol wash. The electrochemically formed polymer was determined to likely be either polyphenylene ether or polyphenylene oxide by SEM and TGA and could be partially removed with the washing step. The insight gained here on the comparison of the three CNT networks and the electrochemical passivation mechanisms will be utilized to extend and optimize the lifetime of anodic CNT networks.

ASSOCIATED CONTENT

Supporting Information

Images of the electrochemical filtration setup and of the CNT filters, SEM images of all CNT networks used in this study at both 50 k× and 100 k× magnification, TGA and multipeak fitted dTG data of all the CNT networks, XPS data of all the CNT networks, and complete electrochemical analysis and effluent composition data for electrochemical filtration experiments run with 0, 0.1, and 1.0 mM influent phenol. This material is available free of charge via the Internet at http://pubs.acs.org/.

AUTHOR INFORMATION

Corresponding Author

*E-mail: vecitis@seas.harvard.edu. Phone: (617) 496-1458.

Notes

The authors declare no competing financial interest.

ACKNOWLEDGMENTS

G.G. thanks the Harvard GSAS Visiting Fellow Scholarship. We thank Dr. Hao-Yu (Greg) Lin for assistance with the XPS analysis. We thank Harvard's Center for Nanoscale Systems for SEM and XPS. We thank Harvard's Material Research Science and Engineering Center for TGA.

REFERENCES

(1) Bard, A. J.; Faulkner, L. R. *Electrochemical Methods: Fundamentals and Applications*, 2nd ed.; John Wiley & Sons: New York, 2001; p 833.
(2) Yang, J.; Wang, J.; Jia, J. P. *Environ. Sci. Technol.* **2009**, *43* (10), 3796−3802.
(3) Martinez-Huitle, C. A.; Brillas, E. *Angew. Chem., Int. Ed.* **2008**, *47* (11), 1998−2005.
(4) Panizza, M.; Cerisola, G. *Chem. Rev.* **2009**, *109* (12), 6541−6569.
(5) Park, H.; Vecitis, C. D.; Choi, W.; Weres, O.; Hoffmann, M. R. *J. Phys. Chem. C* **2008**, *112* (4), 885−889.
(6) Gao, G.; Vecitis, C. D. *Environ. Sci. Technol.* **2011**.
(7) Li, J.; Cassell, A.; Delzeit, L.; Han, J.; Meyyappan, M. *J. Phys. Chem. B* **2002**, *106* (36), 9299−9305.
(8) Tong, X. L.; Zhao, G. H.; Liu, M. C.; Cao, T. C.; Liu, L.; Li, P. Q. *J. Phys. Chem. C* **2009**, *113* (31), 13787−13792.
(9) Vecitis, C. D.; Schnoor, M. H.; Rahaman, M. S.; Schiffman, J. D.; Elimelech, M. *Environ. Sci. Technol.* **2011**, *45* (8), 3672−3679.
(10) Hu, Y. S.; Adelhelm, P.; Smarsly, B. M.; Hore, S.; Antonietti, M.; Maier, J. *Adv. Funct. Mater.* **2007**, *17* (12), 1873−1878.
(11) Brady-Estevez, A. S.; Schnoor, M. H.; Vecitis, C. D.; Saleh, N. B.; Elimelech, M. *Langmuir* **2010**, 14975−14982.
(12) Vecitis, C. D.; Gao, G. D.; Liu, H. *J. Phys. Chem. C* **2011**, *115* (9), 3621−3629.
(13) Liu, H.; Vecitis, C. D. *J. Phys. Chem. C* **2012**, *116*, 374−383.
(14) Bandow, S.; Numao, S.; Iijima, S. *J. Phys. Chem. C* **2007**, *111* (32), 11763−11766.
(15) Carroll, D. L.; Redlich, P.; Blase, X.; Charlier, J. C.; Curran, S.; Ajayan, P. M.; Roth, S.; Ruhle, M. *Phys. Rev. Lett.* **1998**, *81* (11), 2332−2335.
(16) Czerw, R.; Terrones, M.; Charlier, J. C.; Blase, X.; Foley, B.; Kamalakaran, R.; Grobert, N.; Terrones, H.; Tekleab, D.; Ajayan, P. M.; Blau, W.; Ruhle, M.; Carroll, D. L. *Nano Lett.* **2001**, *1* (9), 457−460.
(17) Mukhopadhyay, I.; Hoshino, N.; Kawasaki, S.; Okino, F.; Hsu, W. K.; Touhara, H. *J. Electrochem. Soc.* **2002**, *149* (1), A39−A44.
(18) Wiggins-Camacho, J. D.; Stevenson, K. J. *J. Phys. Chem. C* **2009**, *113* (44), 19082−19090.
(19) Barone, V.; Peralta, J. E.; Uddin, J.; Scuseria, G. E. *J. Chem. Phys.* **2006**, *124* (2), 1−5.
(20) Lee, J. M.; Park, J. S.; Lee, S. H.; Kim, H.; Yoo, S.; Kim, S. O. *Adv. Mater.* **2011**, *23* (5), 629−631.

(21) Wang, R. X.; Zhang, D. J.; Zhang, Y. M.; Liu, C. B. *J. Phys. Chem. B* **2006**, *110* (37), 18267−18271.
(22) Deng, C. Y.; Chen, J. H.; Chen, X. L.; Mao, C. H.; Nie, L. H.; Yao, S. Z. *Biosens. Bioelectron.* **2008**, *23* (8), 1272−1277.
(23) Maldonado, S.; Morin, S.; Stevenson, K. J. *Carbon* **2006**, *44* (8), 1429−1437.
(24) Alexeyeva, N.; Shulga, E.; Kisand, V.; Kink, I.; Tammeveski, K. *J. Electroanal. Chem.* **2010**, *648* (2), 169−175.
(25) Weber, M.; Weber, M. *Phenols*; Springer-Verlag: Berlin, 2010.
(26) http://cumulis.epa.gov/supercpad/cursites/srchsites.cfm.
(27) Kim, U. J.; Furtado, C. A.; Liu, X. M.; Chen, G. G.; Eklund, P. C. *J. Am. Chem. Soc.* **2005**, *127* (44), 15437−15445.
(28) Redlich, P.; Loeffler, J.; Ajayan, P. M.; Bill, J.; Aldinger, F.; Ruhle, M. *Chem. Phys. Lett.* **1996**, *260* (3−4), 465−470.
(29) Cho, H. H.; Smith, B. A.; Wnuk, J. D.; Fairbrother, D. H.; Ball, W. P. *Environ. Sci. Technol.* **2008**, *42* (8), 2899−2905.
(30) Pan, B.; Xing, B. S. *Environ. Sci. Technol.* **2008**, *42* (24), 9005−9013.
(31) Wardman, P. *J. Phys. Chem. Ref. Data* **1989**, *18* (4), 1637−1755.
(32) Ohnuki, Y.; Matsuda, H.; Ohsaka, T.; Oyama, N. *J. Electroanal. Chem.* **1983**, *158* (1), 55−67.
(33) Comninellis, C.; Pulgarin, C. *J. Appl. Electrochem.* **1991**, *21* (8), 703−708.
(34) Iniesta, J.; Michaud, P. A.; Panizza, M.; Cerisola, G.; Aldaz, A.; Comninellis, C. *Electrochim. Acta* **2001**, *46* (23), 3573−3578.
(35) Mengoli, G.; Musiani, M. M. *Electrochim. Acta* **1986**, *31* (2), 201−210.
(36) Park, H.; Vecitis, C. D.; Hoffmann, M. R. *J. Phys. Chem. C* **2009**, *113* (18), 7935−7945.
(37) Datsyuk, V.; Kalyva, M.; Papagelis, K.; Parthenios, J.; Tasis, D.; Siokou, A.; Kallitsis, I.; Galiotis, C. *Carbon* **2008**, *46* (6), 833−840.
(38) Neta, P.; Huie, R. E.; Ross, A. B. *J. Phys. Chem. Ref. Data* **1988**, *17* (3), 1027−1284.
(39) Lim, M.; Han, G. C.; Ahn, J. W.; You, K. S. *Int. J. Environ. Res. Public Health* **2010**, *7* (1), 203−228.
(40) *CRC Handbook of Chemistry and Physics*, 91 ed.; CRC Press: Boca Raton, FL, 2011.